Cu nuclear quadrupole resonance study of substituently induced disorder in $Y_{1-x}Ca_xBa_{2-x}La_xCu_4O_8$

G. V. M. Williams
The MacDiarmid Institute, Industrial Research, P.O. Box 31310, Lower Hutt 5040, New Zealand
(Received 8 May 2007; revised manuscript received 23 July 2007; published 5 September 2007)

Cu nuclear quadrupole resonance (NQR) measurements have been made on $Y_{1-x}Ca_xBa_{2-x}La_xCu_4O_8$ to study the effects of disorder on the electronic state in samples where codoping with Ca and La ensures that there is no large change in the number of doped holes per Cu. It is found that there is a systematic increase in the static charge disorder induced by codoping. There is also a small increase in the Cu spin-lattice relaxation rate $1/^{63}T_1$ for temperatures above the superconducting transition temperature T_c, which can be accounted for by a small decrease in the normal-state pseudogap energy. $1/^{63}T_1$ does not follow the expected T^{-3} temperature dependence for temperatures far below T_c, which may be a consequence of the inhomogeneous electronic state. However, there is no evidence that codoping induced disorder leads to any reduction in the Cu NQR intensity for temperatures above T_c, even though the average hole concentration is close to the boundary where a reduction in the Cu NMR intensity might be expected.

DOI: 10.1103/PhysRevB.76.094502 PACS number(s): 74.72.−h, 74.25.Nf, 74.20.Mn

INTRODUCTION

There have been a number of reports of a partial or complete reduction in the Cu nuclear magnetic resonance (NMR) and nuclear quadrupole resonance (NQR) intensities in the $La_{2-x}Sr_xCuO_4$ and $Y_{1-x}Ca_xBa_2Cu_3O_{7-\delta}$ families of high temperature superconducting cuprates (HTSCs) as the temperature is decreased, which commences when the number of doped holes per copper is less than ~ 0.13.[1–5] A complete loss also occurs for certain values of x and y in $La_{2-x-y}(Nd,Eu)_ySr_xCuO_4$,[6–10] and a partial loss occurs in $Sr_{0.9}La_{0.1}CuO_2$ (Ref. 11) and $Pr_{2-x}Ce_xCuO_4$ (Ref. 12) for $x < 0.13$. This reduction or wipeout has been attributed to effects that include charge-stripe order[9] or an inhomogeneous slowing down of the spin dynamics.[6] The dynamic inhomogeneities have been observed in inelastic neutron scattering measurements,[13–16] and they have been interpreted in terms of dynamic phase separation into hole-rich and hole-poor regions.[17–19]

The effect of a slowing down of the spin or charge dynamics on the Cu NMR intensity can be understood by noting that when the characteristic spin or charge fluctuation rate decreases, it will lead to a large increase in the Cu spin-lattice relaxation rate $1/T_1$ that will be maximized when the fluctuation rate is comparable to the NMR or NQR frequency. This effect is well known in magnetically ordered systems where $1/T_1$ dramatically increases as the temperature is reduced toward the magnetic ordering temperature.[20,21] For Cu in the HTSCs, the Cu spin-lattice relaxation time can become comparable or smaller than the time between the $\tau_{\pi/2}$ and τ_π pulses leading to a reduction in the detected Cu NMR intensity. There have been reports that the Cu NMR signal is partially recovered at low temperatures where the spin and charge inhomogeneities are static on the NMR and NQR time scales.[6,22,23]

While there are different mechanisms that can lead to a slowing down of the spin and charge dynamics, it is has been argued that the slowing down occurs inhomogeneously with decreasing temperature.[7] It is possible that static disorder induced by the dopant atoms[2,24] can lead to a pinning of the dynamic inhomogeneities and thus lead to the observed reduction and wipeout of the Cu NMR intensity with decreasing temperature. It should also be noted that there is evidence for very short range charge and spin inhomogeneities.[25,26] Since the reduction or wipeout of the Cu NMR intensity is doping dependent,[1–5] it is important to study samples where structural and charge disorder can be induced without a large change in the average hole concentration. For this reason, NQR measurements were made on $Y_{1-x}Ca_xBa_{2-x}La_xCu_4O_8$ that was codoped with Ca and La, and the results are reported in this paper.

$Y_{1-x}Ca_xBa_{2-x}La_xCu_4O_8$ was chosen for this study because ideally, hole doping by Ca should be canceled by electron doping by La. Ca substitutes for Y that is between the two CuO_2 planes, and La substitutes for Ba that is between a CuO_2 plane and a CuO filled chain. Thus, substitutional disorder can be studied without any major hole doping effects. The hole concentration p in the parent compound ($p \sim 0.12$ doped holes per Cu) is also near the hole concentration boundary where a reduction of the Cu NMR and NQR intensities is observed in $La_{2-x}Sr_xCuO_4$ and $Y_{1-x}Ca_xBa_2Cu_3O_{7-\delta}$ ($p < 0.13$).[2] It should be noted that there is no evidence for a similar reduction of the Cu NMR and NQR intensities in the pure compound. However, there is the possibility that the introduction of structural and electronic disorder might induce a reduction and localized pinning of dynamic inhomogeneity. However, we show below that there is Ca and La induced charge disorder, but there is no evidence for a reduction in the Cu NQR intensity that could signal pinning of the dynamic inhomogeneities.

EXPERIMENTAL DETAILS

The samples were synthesized from a stoichiometric mix of Y_2O_3, $CaCO_3$, $Ba(NO_3)_2$, La_2O_3, and CuO. This was decomposed in air at 700 °C and then the powder was ground and pressed into pellets. It was followed by reactions at 910,

930, and 945 °C in O_2 at 60 bar with intermediate grinding and pressing into pellets. The phase purity was confirmed by x-ray diffraction measurements. The superconducting transition temperature T_c was measured using a superconducting quantum interference device magnetometer. The T_c values were 81, 86.5, 85, 88.5, and 88 K for $x=0$, 0.03, 0.05, 0.10, and 0.15, respectively. The small increase in T_c indicates that there is some initial doping effect that has saturated for $x \geqslant 0.03$.

All the Cu nuclear quadrupole resonance (NQR) measurements, except the Cu NQR intensity measurements, were made using a homebuilt NQR apparatus with a mu-metal shield and powder samples as previously described.[27] The Cu NQR spectra were obtained using a Hahn echo sequence, $\tau_{\pi/2}$-τ-τ_{π}-τ, where $\tau_{\pi/2}$ was between 1.5 and 2 μs and the time between the $\pi/2$ pulse and the π pulse, τ, was 9–10 μs. The spectra were obtained by Fourier transforming the second half of the echo and then summing the spectra measured at discrete frequencies.

The Cu spin-lattice relaxation rate was obtained using an inversion recovery pulse sequence, τ_{π}-τ_1-$\tau_{\pi/2}$-τ-τ_{π}-τ, where $\tau_{\pi/2}$ was between 1.5 and 2 μs. $1/^{63}T_1$ was obtained by fitting the magnetization recovery $M(\tau_1)$ to

$$M(\tau_1) = M_0[1 - 2\exp(-3\tau_1/^{63}T_1)]. \quad (1)$$

The additional factor of 3 is added in order to enable a direct comparison between the NQR and NMR spin-lattice relaxation rates.

Cu NQR intensity measurements were made using a TecMag spectrometer. The NQR spectra were taken using the point-by-point method and a Hahn echo sequence where the pulses $\tau_{\pi/2}$ and τ_{π} were 6 and 12 μs, respectively, and τ was 13 μs. This resulted in a Fourier transformed spin-echo linewidth that was much less than the linewidths of the spectrum being measured. The intensity at each frequency was obtained by integrating the spin echo. Since the spin-echo intensity is a function of τ, the spin-echo intensity must be extrapolated back to $\tau=0$. This was done using a Hahn echo sequence by varying τ and integrating the spin echo. For the HTSCs, the magnetization can be expressed as

$$M(\tau) = M_0 \exp\left(-\frac{2\tau}{T_{2R}}\right)\exp\left(-\frac{1}{2}\frac{(2\tau)^2}{T_{2g}^2}\right). \quad (2)$$

The first factor is the Redfield contribution and it is related to the spin-lattice relaxation process. For $YBa_2Cu_4O_8$, it has been shown that $T_{2R}^{-1}=5.6T_1^{-1}$ when obtained using NQR.[28] The second factor is a Gaussian decay function, where T_{2g} is the Gaussian spin-spin relaxation time. It arises from electron mediated indirect nuclear spin-spin couplings between neighboring Cu spins having the same Larmor frequency.[29,30] However, it was not possible to fit the data to Eq. (2) using the measured T_1 values and a full Gaussian component. This is an unavoidable consequence of using a narrow excitation range that does not lead to an artificial broadening of the Cu NQR spectrum. For this reason, we used Eq. (2) to fit the spin-spin magnetization data and an additional exponential factor, $\exp(-2\tau/T_{2L})$.

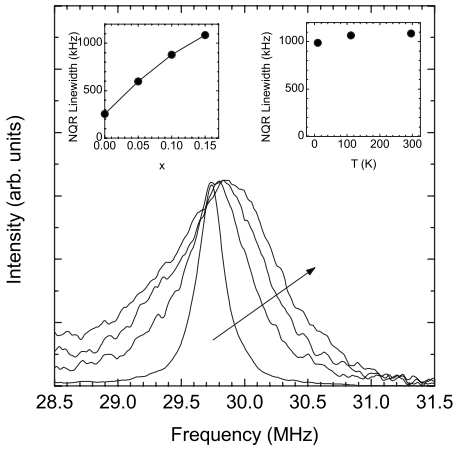

FIG. 1. Plot of the room temperature Cu NQR spectra from $Y_{1-x}Ca_xBa_{2-x}La_xCu_4O_8$ for x values of 0, 0.05, 0.10, and 0.15. The arrow indicates increasing x. Left inset: Plot of the ^{63}Cu NQR linewidth against x. Right inset: Plot of the ^{63}Cu NQR linewidth against temperature for $x=0.15$.

The intensity comparisons for all samples were made using a rigid coil made from Manganin wire embedded in epoxy. The Manganin wire ensured that the coil resonance width was large and that the Q_r of the coil was only weakly temperature dependent and not affected by the sample over the measured temperature range. Thus, only a small change in the rf power was required to maintain the same $\tau_{\pi/2}$ at all temperatures. The Q_r was measured using a network analyzer. The samples were finely ground and placed in quartz tubes where the sample length was enclosed within the coil. The spectra were also corrected for the Boltzmann factor and the sample mass.

RESULTS AND ANALYSIS

It is apparent in Fig. 1 that there is an increase in the ^{63}Cu NQR linewidth with increasing x. Here, we only plot the ^{63}Cu NQR spectra from the CuO_2 planes because we were limited by the tuning range of the coil. The ^{65}Cu NQR spectra occur at a lower frequency and intensity. The resultant ^{63}Cu NQR linewidths are plotted in the left inset of Fig. 1. The data in Fig. 1 can be understood by noting that the Cu NQR frequency ν_Q in the HTSCs is given by $\nu_Q = [(eQV_{zz})/(2h)]\sqrt{1+\eta^2/3}$, where V_{zz} is the maximum principle component of the electric-field-gradient tensor, eQ is the nuclear electric quadrupole moment, and η is the asymmetry parameter given by $\eta=(V_{xx}-V_{yy})/V_{zz}$, with $|V_{zz}| \geqslant |V_{yy}| \geqslant |V_{xx}|$. The electric-field-gradient principal axis is along the c axis and hence η is zero for Cu in the CuO_2 plane,[31] which leads to $\nu_Q=(eQV_{zz})/(2h)$.

ν_Q has experimentally been observed to correlate with p in the HTSCs.[26,32,33] For example, $\nu_Q=33+18p$ in $La_{2-x}Sr_xCuO_4$. It has recently been argued that this correlation is predominately due to two effects: holes in the $3d_{x^2-y^2}$ orbital and virtual hopping from the neighboring oxygen to the unoccupied Cu $4p$ orbital.[33] The contribution from the distant ions is small and it has been estimated to contribute

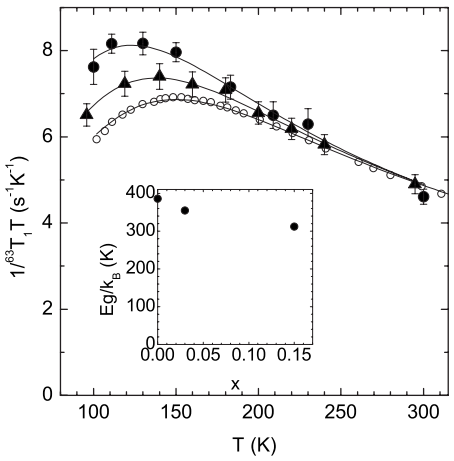

FIG. 2. Plot of $1/^{63}T_1T$ against temperature for $Y_{1-x}Ca_xBa_{2-x}La_xCu_4O_8$ with $x=0$ [open circles (Ref. 34)], $x=0.03$ (filled triangles), and $x=0.15$ (filled circles). The solid curves are fits to the data using Eq. (4) that includes a normal-state pseudogap factor and a spin-fluctuation factor. Inset: Plot of the fitted pseudogap energy against x.

only 2.59 MHz to the $La_{2-x}Sr_xCuO_4$ NQR frequency. Thus, any local charge disorder will lead to a distribution in V_{zz} that will lead to an increase in the Cu NQR linewidth. Therefore, it is possible that the increase in the Cu NQR linewidth arises from charge disorder induced by the Ca and La cosubstitution. From the correlation between ν_Q and p found in $La_{2-x}Sr_xCuO_4$, it is possible to estimate that the linewith for $Y_{0.85}Ca_{0.15}Ba_{1.85}La_{0.15}Cu_4O_8$ corresponds to $\Delta p=\pm 0.03$. This is approximately $\frac{1}{2}$ of the Δp estimated from the ^{63}Cu NQR data in $La_{2-x}Sr_xCuO_4$, where the charge distribution was attributed to nonuniform doping by Sr.[24] The small increase in the ^{63}Cu NQR frequency seen in Fig. 1 corresponds to an increase in p of no more than 0.007.

There is no evidence that the static charge distribution changes with temperature. This can be seen in the right inset of Fig. 1, where the ^{63}Cu NQR linewidth is plotted for $Y_{0.85}Ca_{0.15}Ba_{1.85}La_{0.15}Cu_4O_8$ to low temperatures. The ^{63}Cu NQR linewidth is nearly independent of temperature, which suggests that the underlying charge distribution is also independent of temperature. In particular, there is no large increase in the ^{63}Cu NQR linewidth at low temperatures that has been reported in some HTSCs, which has been attributed to the high temperature inhomogeneous spin and charge dynamics that have sufficiently slowed at low temperatures so that they appear static on the NMR and NQR time scales.[6,22,23]

The spin-lattice relaxation rate data are plotted in Fig. 2 for $Y_{1-x}Ca_xBa_{2-x}La_xCu_4O_8$ with $x=0$, $x=0.03$, and $x=0.15$ as $1/^{63}T_1T$. In overdoped HTSCs, where the normal-state pseudogap is small, it has been argued that the increase in $1/^{63}T_1T$ with decreasing temperature is due to antiferromagnetic spin fluctuations.[32,34,35] These will affect $1/^{63}T_1T$ because for metallic and magnetic systems, the magnetic relaxation rate can be written as[36]

$$(T_1T)^{-1}=\frac{1}{2}\hbar k_B\gamma_n^2\sum_{\mathbf{q}}|A(\mathbf{q})|^2\frac{\chi''(\mathbf{q},\omega_0)}{\hbar\omega_0}, \quad (3)$$

where ω_0 is the NMR angular frequency, $|A(\mathbf{q})|$ is the form factor containing the hyperfine coupling constants, and $\chi''(\mathbf{q},\omega_0)$ is the imaginary part of the dynamical spin susceptibility. Using the hyperfine coupling model applied to the HTSCs,[37] it can be shown that $|A(\mathbf{q})|$ is peaked at the antiferromagnetic wave vector.

It is possible to use the dynamical spin susceptibility of Millis *et al.*[35] and the assumed temperature dependence of the antiferromagnetic correlation length[38] to predict from Eq. (3) that $1/^{63}T_1T=a_0\vartheta/(T+\vartheta)$, where a_0 and ϑ are constants. This is the temperature dependence found in overdoped HTSCs.[34] The presence of a pseudogap in the underdoped and hole-doped HTSCs[39] leads to a departure from this temperature dependence.[41] The pseudogap can be accounted for by writing $1/^{63}T_1T$ as $1/^{63}T_1T=[a_0\vartheta/(T+\vartheta)]P$, where P is a function that decreases with decreasing temperature. Using a triangular density of states for the normal-state pseudogap in $YBa_2Cu_4O_8$, it is possible to fit the $1/^{63}T_1T$ data to

$$1/^{63}T_1T=[a_0T_0/(T+T_0)]\{1-(2k_BT/E_g)\times[\tanh(E_g/2k_BT)]^z\ln(\cosh(E_g/2k_BT))\}, \quad (4)$$

where E_g is the pseudogap energy, k_B is the Boltzmann constant, and $z=4.55$.[42]

It can be seen in Fig. 2 that Eq. (4) provides a good fit to the data where $a_0=66$ s^{-1} K^{-1} and $T_0=25$ K for all x values in the figure. The fitted values of E_g are plotted in the inset of Fig. 2, where it can be seen that there is a small decrease in E_g with increasing x. This may be due to the small doping effect mentioned earlier. However, the data clearly show that the charge disorder induced by Ca and La codoping does not have a significant effect on the spin dynamics as probed by $1/^{63}T_1T$. Furthermore, the spin-lattice magnetization recovery above T_c could be fitted to a single $^{63}T_1$. This can be compared with materials that show spin disorder that leads to a distribution in $^{63}T_1$.[7,24,43] Thus, our data are also consistent with the absence of a significant spatial distribution in the spin-fluctuation spectrum above T_c.

The $1/^{63}T_1$ data below T_c for $x=0.15$ (Fig. 3) do not show the temperature dependence found in the pure sample. We first note that the magnetization recovery could not be fitted to a single $1/^{63}T_1$. This implies a distribution in $1/^{63}T_1$ that has been observed in other compounds when the electronic state is spatially inhomogeneous.[7,24,43] In this situation where there is no specific model for the $1/^{63}T_1$ distribution, the magnetization recovery can be fitted to

$$M(\tau)=M_0[1-2\exp(-[3\tau/^{63}T_1]^n)]. \quad (5)$$

The resultant exponent n is plotted in the inset of Fig. 3, and it can be seen that it systematically decreases below T_c. The departure from a single $1/^{63}T_1$ is unlikely to be due to fluxoids because n for the pure compound is 1 below ~40 K.[40]

For a Fermi liquid and in the absence of spin fluctuations, it is possible to show that $1/^{63}T_1$ is proportional to $T\int N(E)f(E)[1-f(E)]dE$, where $N(E)$ is the density of states and $f(E)$ is the Fermi function. For a d-wave superconductor,

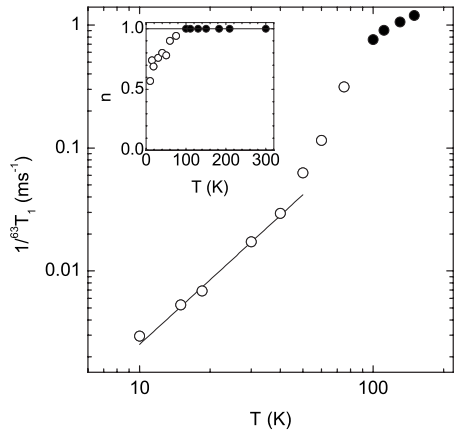

FIG. 3. Plot of $1/^{63}T_1$ against temperature from $Y_{0.85}Ca_{0.15}Ba_{1.85}La_{0.15}Cu_4O_8$ below (open circles) and above (filled circles) T_c. The curve is a best fitted to $1/^{63}T_1=a_1T^{-m}$. Inset: Plot of the stretched exponential exponent used to fit the magnetization recovery with Eq. (5) against temperature.

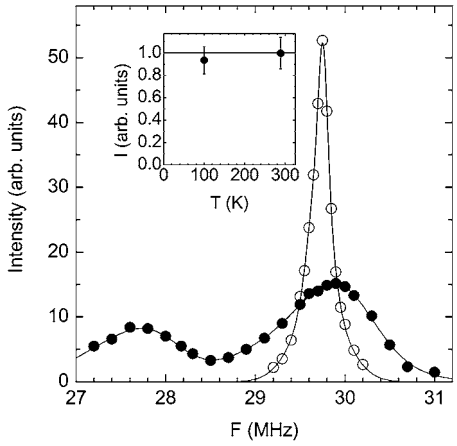

FIG. 4. Plot of the Cu NQR spectra from $Y_{1-x}Ca_xBa_{2-x}La_xCu_4O_8$ at 100 K with $x=0$ (open circles) and $x=0.15$ (filled circles). The solid curves are multiple Gaussian fits to the data as described in the text. The data have been corrected for the mass and Q_r. Inset: Plot of the integrated ^{63}Cu NQR intensity against temperature for $YBa_2Cu_4O_8$ and scaled to the high temperature value. The data were corrected for mass, Q_r, and the spin-echo decay.

it is easy to show that $1/^{63}T_1=a_1T^{-m}$ at low temperatures where m is 3.[40] This has been found in pure $YBa_2Cu_4O_8$ (Ref. 40) and $YBa_2Cu_3O_7$ (Ref. 32) at low temperatures. However, a value of m close to 1 has been reported from measurements on $La_{2-x}Sr_xCuO_4$ (Ref. 32) that is known to have extensive charge disorder, where Δp can be as large as 0.06 and increases with decreasing temperature.[24] It can be seen in Fig. 3 that the low temperature $Y_{0.85}Ca_{0.15}Ba_{1.85}La_{0.15}Cu_4O_8$ data can be fitted to $1/^{63}T_1=a_1T^{-m}$ with $m=1.74$, which is clearly below the value expected for a spatially homogeneous d-wave superconductor. This departure could be a consequence of spatial inhomogeneities.

There is no evidence that the disorder induced by Ca and La cosubstitution leads to any reduction in the Cu NQR intensity at 100 K. This can be seen in Fig. 4 where the Cu NQR spectra are plotted at 100 K for $Y_{1-x}Ca_xBa_{2-x}La_xCu_4O_8$ with $x=0$ and $x=0.15$ after the mass and Q_r corrections. The $x=0$ ^{63}Cu NQR spectra are narrow and do not overlap the ^{65}Cu NQR spectra, and hence, only the ^{63}Cu NQR spectra are shown. The solid curve is a three-Gaussian fit to the data. The $x=0.15$ spectra are broad, and the ^{63}Cu and ^{65}Cu NQR peaks overlap. The spectra were fitted to four Gaussians to represent the broad and asymmetric ^{63}Cu and ^{65}Cu NQR peaks. The best fit is shown in Fig. 4, and the ^{63}Cu and ^{65}Cu peaks have the intensity ratios expected from the isotropic abundance. The fitted ^{63}Cu NQR intensity was corrected for the fact that the data were taken at a finite τ, and the intensity at $\tau=0$ was estimated by measuring $M(\tau)$ as a function of τ at the peak frequency. This was fitted to Eq. (2) with the additional $\exp(-2\tau/T_{2L})$ factor and the intensity extrapolated back to $\tau=0$. This resulted in a ^{63}Cu NQR intensity of 1 ± 0.12 for $x=0$ and 0.96 ± 0.14 for $x=0.15$, where the intensities were scaled by the mean value for $x=0$. These values are equal within the experimental uncertainly.

The ^{63}Cu NQR intensity of $YBa_2Cu_4O_8$ was also measured as a function of temperature above T_c, and the results can be seen in the inset of Fig. 4. It is apparent that there is no loss of the ^{63}Cu NQR intensity within the experimental uncertainty.

CONCLUSION

In conclusion, cosubstitution by Ca and La in $Y_{1-x}Ca_xBa_{2-x}La_xCu_4O_8$ only leads to a small change in the average hole concentration as estimated from the T_c values. However, there is a systematic increase in the ^{63}Cu NQR linewidths that can be interpreted in terms of charge disorder that increases with increasing x. There is no evidence for a concomitant spatial variation in the spin-fluctuation spectrum as probed by $1/^{63}T_1T$ above T_c. Below T_c, there is a spatial distribution in $1/^{63}T_1$ that may arise from inhomogeneous spin dynamics. It is found that the spatially induced disorder above T_c does not lead to a reduction in the Cu NQR intensity even though $YBa_2Cu_4O_8$ has a hole concentration close to that where a reduction in the Cu NQR intensity might be expected based on measurements on some of the other HTSCs.

ACKNOWLEDGMENTS

We acknowledge useful discussions with J. Haase and thank B. Büchner from the IFW for access to the NMR facilities. The assistance by S. Krämer with some of the measurements is gratefully acknowledged. The provision of one sample by J. Storey and x-ray diffraction measurements by S. Goh are also gratefully acknowledged. Funding support was provided by the New Zealand Marsden Fund, the New Zealand Foundation for Research Science and Technology, and the Alexander von Humboldt Foundation.

[1] M.-H. Julien, A. Campana, A. Rigamonti, P. Carretta, F. Borsa, P. Kuhns, A. P. Reyes, W. G. Moulton, M. Horvatic, C. Berthier, A. Vietkin, and A. Revcolevschi, Phys. Rev. B **63**, 144508 (2001).
[2] P. M. Singer and T. Imai, Phys. Rev. Lett. **88**, 187601 (2002).
[3] Y. Kobayashi, T. Miyashita, M. Ambai, T. Fukamachi, and M. Sato, J. Phys. Soc. Jpn. **70**, 1133 (2001).
[4] A. W. Hunt, P. M. Singer, K. R. Thurber, and T. Imai, Phys. Rev. Lett. **82**, 4300 (1999).
[5] J. Haase (private communication).
[6] A. W. Hunt, P. M. Singer, A. F. Cederström, and T. Imai, Phys. Rev. B **64**, 134525 (2001).
[7] N. J. Curro, P. C. Hammel, B. J. Suh, M. Hücker, B. Büchner, U. Ammerahl, and A. Revcolevschi, Phys. Rev. Lett. **85**, 642 (2000).
[8] T. Sawa, M. Matsumura, and H. Yamagata, J. Phys. Soc. Jpn. **70**, 3503 (2001).
[9] P. M. Singer, A. W. Hunt, A. F. Cederström, and T. Imai, Phys. Rev. B **60**, 15345 (1999).
[10] G. B. Teitel'baum, I. M. Abu-Shiekah, O. Bakharev, H. B. Brom, and J. Zaanen, Phys. Rev. B **63**, 020507(R) (2000).
[11] G. V. M. Williams and J. Haase, Phys. Rev. B **75**, 172506 (2007).
[12] G. V. M. Williams, J. Haase, Min-Seok Park, Kyung Hee Kim, and Sung-Ik Lee, Phys. Rev. B **72**, 212511 (2005).
[13] K. Yamada, C. H. Lee, K. Kurahashi, J. Wada, S. Wakimoto, S. Ueki, H. Kimura, Y. Endoh, S. Hosoya, G. Shirane, R. J. Birgeneau, M. Greven, M. A. Kastner, and Y. J. Kim, Phys. Rev. B **57**, 6165 (1998).
[14] J. M. Tranquada, J. D. Axe, N. Ichikawa, A. R. Moodenbaugh, Y. Nakamura, and S. Uchida, Phys. Rev. Lett. **78**, 338 (1997).
[15] H. A. Mook and P. Dai, Nature (London) **404**, 729 (2000).
[16] P. Dai, H. A. Mook, and F. Dogan, Phys. Rev. Lett. **80**, 1738 (1998).
[17] S. R. White and D. J. Scalapino, Phys. Rev. B **61**, 6320 (2000).
[18] V. J. Emery, S. A. Kivelson, and H. Q. Lin, Phys. Rev. Lett. **64**, 475 (1990).
[19] V. J. Emery, E. Fradkin, S. A. Kivelson, and T. C. Lubensky, Phys. Rev. Lett. **85**, 2160 (2000).
[20] T. Moriya, Prog. Theor. Phys. **16**, 23 (1956).
[21] G. Allodi, M. Cestelli Guidi, R. De Renzi, A. Caneiro, and L. Pinsard, Phys. Rev. Lett. **87**, 127206 (2001).
[22] M. Matsumura, T. Ikeda, and H. Yamagata, J. Phys. Soc. Jpn. **69**, 1023 (2000).
[23] G. B. Teitel'baum, B. Büchner, and H. de Gronckel, Phys. Rev. Lett. **84**, 2949 (2000).
[24] P. M. Singer, A. W. Hunt, and T. Imai, Phys. Rev. Lett. **88**, 047602 (2002).
[25] J. Haase, C. P. Slichter, and C. T. Milling, J. Supercond. **15**, 339 (2002).
[26] J. Haase and G. V. M. Williams, Curr. Appl. Phys. **6**, 293 (2006).
[27] S. Krämer and M. Mehring, Phys. Rev. Lett. **83**, 396 (1999).
[28] R. L. Corey, N. J. Curro, K. O'Hara, T. Imai, C. P. Slichter, K. Yoshimura, M. Katoh, and K. Kosuge, Phys. Rev. B **53**, 5907 (1996).
[29] C. H. Pennington, D. J. Durand, C. P. Slichter, J. P. Rice, E. D. Bukowski, and D. M. Ginsberg, Phys. Rev. B **39**, 274 (1989).
[30] C. H. Pennington and C. P. Slichter, Phys. Rev. Lett. **66**, 381 (1991).
[31] H. Zimmermann, M. Mali, D. Brinkmann, J. Karpinski, E. Kaldris, and S. Rusiecki, Physica C **159**, 681 (1989).
[32] For a review, see K. Asayama, Y. Kitaoka, G. Q. Zheng, and K. Ishida, Prog. Nucl. Magn. Reson. Spectrosc. **28**, 221 (1996).
[33] J. Haase, O. P. Sushkov, P. Horsch, and G. V. M. Williams, Phys. Rev. B **69**, 094504 (2004).
[34] F. Raffa, T. Ohno, M. Mali, J. Roos, D. Brinkmann, K. Conder, and M. Eremin, Phys. Rev. Lett. **81**, 5912 (1998).
[35] A. J. Millis, H. Monien, and D. Pines, Phys. Rev. B **42**, 167 (1990).
[36] T. Moriya, J. Phys. Soc. Jpn. **18**, 516 (1963).
[37] B. S. Shastry, Phys. Rev. Lett. **63**, 1288 (1989); F. Mila and T. M. Rice, Physica C **157**, 561 (1989).
[38] T. Imai, C. P. Slichter, A. P. Paulikas, and B. Veal, Phys. Rev. B **47**, 9158 (1993).
[39] M. Mehring, Appl. Magn. Reson. **3**, 383 (1992).
[40] M. Bankay, M. Mali, J. Roos, and D. Brinkmann, Phys. Rev. B **50**, 6416 (1994).
[41] G. V. M. Williams, J. L. Tallon, and J. W. Loram, Phys. Rev. B **58**, 15053 (1998).
[42] G. V. M. Williams, D. J. Pringle, and J. L. Tallon, Phys. Rev. B **61**, R9257 (2000).
[43] Y. Itoh, T. Machi, N. Koshizuka, M. Murakami, H. Yamagata, and M. Matsumura, Phys. Rev. B **69**, 184503 (2004).